2020 16th IEEE International Conference on Automation Science and Engineering (CASE)
August 20-21, 2020, Online Zoom Meeting

Model-Based Suppression Control for Liquid Vessels Carried by a Humanoid Robot While Stair-Climbing

Jean Chagas Vaz[1] and Paul Oh[2]

Abstract— **This paper presents a study to evaluate the effects of sloshing phenomena while a humanoid robot climbs stairs while carrying water containers. Currently humanoid robots can perform a wide range of tasks including handling tools, climbing ladders, and patrolling rough terrain. However, when it comes to manipulation of objects humanoids are fairly limited. This becomes more apparent when humanoids have to handle non-rigid objects. Although many full-sized humanoids cost an extensive amount of money, they fail to respond to common tasks during disaster relief such as delivering water to the victims or possible fires. After disasters such as Hurricane Maria, the need for humanoid robots to assist in these scenarios is becoming increasingly evident. In previous work the authors have developed an algorithm which allows the robot to walk while carrying water buckets. Experiments conducted use the full-sized humanoid DRC-Hubo as an experimental platform. Moreover, a sloshing reduction controller is implemented in order to suppress rocking disturbances. The system was integrated via ROS (Robot Operating System). Additionally, the sloshing reduction was evaluated based on sensor data evaluation.**

I. INTRODUCTION

Natural disasters like hurricane Maria impacts thousands of lives. Puerto Rico was one of the most inflicted islands during the hurricane landfall, experiencing island-wide power outages and lack of drinkable water and food [1]. Consequently, Robotics engineers are working fearlessly to improve and create a state-of-the-art technology able to assist humans in case of emergencies. In 2015 the Defense Advanced Research Projects Agency (DARPA) sought to display advanced technology in disaster response [2]. Robots such as NimbRo, CHIMP and DRC-Hubo were some of the highlights of the competition [3][4][5]. Even though, the robots showcased impressive locomotion, navigation, and manipulation abilities, only rigid items were considered for manipulation during the competition. Therefore these humanoids would not be very useful if they had to carry supplies like water and food.

Handling semi-rigid materials such as a body of water confined into a container is a tremendous problem to be tackled. Due, to the sloshing effect the object is constantly subjected to acceleration and deceleration due to the external forces, also known as nonlinear fluid dynamics. For a humanoid robot to carry such an object it has to compensate and mitigate the disturbance caused by the semi-rigid object (vessel and the liquid inside). Otherwise, the ZMP (Zero Moment Point) might shift off the support polygon yielding costly and catastrophic consequences. Therefore, we seek to improve a humanoid's manipulation ability so it can deliver liquid containers in the aftermath of natural disasters, construction sites and war zones. Although, these scenarios present challenges such as rough terrain, obstacles, and staircases, the latter is the main focus of this research (Fig.1). Stair-climbing has been chosen due its deterministic characteristics, such as known dimensions, surface texture, etc. Hence, it is appropriate to implement our controller without worrying about other unmodeled scenarios (e.g. hill slope, foot-floor friction, rugged-terrain).

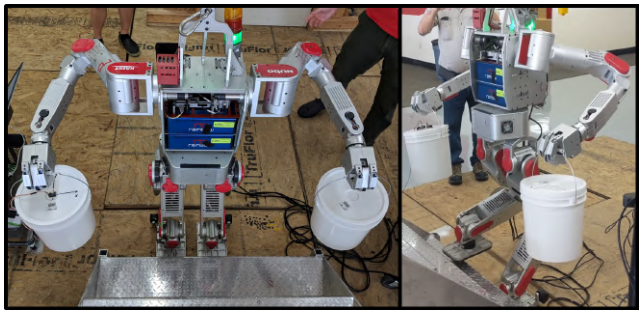

Fig. 1: DRC-Hubo climbing stairs while holding two water containers

This paper is divided in six sections. Section II will describe the related work that: studies disaster response humanoids, presents robotic platforms that performed non-rigid object manipulation, discusses with more focus research that tackled robots handling water vessels, and examines sloshing dynamics and sloshing suppression. Section III will scrutinize the derivation of a spherical pendulum mathematical model by using the sloshing dynamics theory. Furthermore, it will analyze the sloshing suppression controller, and the system integration. Section IV will discuss the chosen robotic platform, as well as the hardware characteristic and experimentation procedures. Section V will showcase results of testing and evaluating of the proposed solution. Finally, Section VI will conclude and present future envisioned work.

II. RELATED WORK

A majority of the literature surrounding humanoid robotic manipulation involves rigid item manipulation. For instance, Shin *et. al.* [6] used a virtual dynamic model based controller to enable the humanoid Mahru to handle a ball in a human-like fashion. Furthermore, the authors focused on dual-arm

Jean C. Vaz is with the Department of Mechanical Engineering, University of Nevada Las Vegas (UNLV), Las Vegas, Nevada 89119, USA. chagasva@unlv.nevada.edu

[2]Paul Oh is with Faculty of Mechanical Engineering, University of Nevada Las Vegas (UNLV), Las Vegas, Nevada 89119, USA. IEEE Member, direct all correspondence to this author, paul.oh@unlv.edu

Authorized licensed use limited to: INDIAN INSTITUTE OF TECHNOLOGY ROORKEE. Downloaded on February 15,2021 at 10:02:51 UTC from IEEE Xplore. Restrictions apply.

manipulation. While handling rigid objects the behaviors of such items can be predicted and modeled whereas if the object is uneven the modeling becomes much more convoluted. When it comes to non-rigid object manipulation such as: sandbags fetching, fire hose handling, laundry folding, and bedridden patients nursing care few studies have been performed.

Alpizar *et. al.* [7] use the humanoid robot HRP-2 to carry a fire hose which can be considered a semi-rigid object. In order to handle the hose the authors implemented a hybrid controller on the robots wrist, and an impedance controller was used to pull the hose which improved the robot's balance. The authors utilized a walking pattern generator that allowed the robot to self-balance while walking, as well as computing the foot transitions and the center of mass trajectory. Finally, Alpizar *et. al.* [7] simulate the dynamics of the hose and the HRP-2 robot on OpenHRP. Their results were satisfactory, and future studies will investigate force feedback to balance. In contrast, Miller *et. al.* [8] studied towel folding by the PR2 robotic platform. Cloth is a very convoluted non-rigid material due to its high flexibility, anti stretchable, and low slip. The authors presented an algorithm which obtains the 2D cloth polygon and utilizes the gravity-fold approach along to fold the clothes. The PR2 robot was able to fold towels on a 200 s average and with a 100% success rate.

The main goal of this research is to tackle the sloshing phenomena of a non-rigid body contained inside a rigid vessel. Most of the research being done on sloshing suppression uses a single robotic arm, instead of a full-sized humanoids[9][10][11][12]. Aribowo *et. al.* [10] investigated the sloshing suppression for point to point motion in a three-dimensional working space, aiming to improve fluid canister handling by service robots. The authors have approached the problem by using cubic spline algorithms and optimization schemes in order to reduce vibrations. Furthermore, a spherical pendulum model was implemented, and in order to simulate the response of the trajectory a numerical sloshing simulation model was utilized[10]. By using the Mitsubishi PA 10-7C robot arm as an experimental platform Aribowo *et. al.* could reduce the sloshing of small vessels by approximately 73% up to 78% [10]. Although an impressive sloshing reduction, this research aims to carry higher quantities of water with a full-size humanoid robot.

Reyhanoglu *et. al.* [11] address liquid sloshing dynamics by using a multi-mass-spring model. This research employs a PPR robot (3-DoF Prismatic-Prismatic-Revolute robot) which is controlled through Lyapunov-based feedback controllers. Once again the primary goal here is a fast robotic delivery of an open container of liquid towards service robots[11]. The authors successfully simulated the convergence of the slosh states to reach rapid equilibrium. Sloshing effects can be a constant problem when being handled by service robots. This phenomena becomes even more significant when it comes to full-sized bipedal robots due to their fragile stability. Another example involves manipulation of biochemical and other hazardous liquids using an industrial robotics arm. Moriello *et. al.* [12] sought to reduce sloshing through vibration suppression for a second order system by using a spherical pendulum mechanical model. The authors utilized a feed-forward approach to mitigate sloshing via the Comau Smart5 Six industrial manipulator[12]. In addition, the robot arm was evaluated while carrying 2 litres of water. The authors pointed out that while there is movement caused by the robot, the liquid inside of the receptacle moves accordingly due to its inertia. Therefore, the sloshing effect can only be analyzed after the robot has come to a full stop.

The authors' previous work tackles non-rigid manipulation while walking without considering the overall sloshing effect[13]. In this paper, a sloshing suppression controller applied to a full-sized humanoid is presented. Sloshing dynamics studies are fairly common, and many models have been studied and designed. Mishra *et. al.* [14] presented a second-order sliding mode control based on the super-twisting algorithm for slosh suppression. Furthermore, they successfully increase the controller's overall robustness by implementing output-feedback control based on a linear surface, and simulation was conducted via MATLAB[14]. For a more experimental approach Purnomo *et. al.* [15] built a sliding table to test a simple pendulum sloshing model in an opened vessel. Their approach resembles a vibration model system by adding a dampener system for the viscosity as well as the friction of fluid. For the controller they used an Active Force Control (AFC) method in order to suppress the system's disturbances[15]. Once again MATLAB simulations were implemented using a custom PID controller to ensure an adequate representation of the dynamic lateral spillage. Conversely, Zang *et. al.* [16] used two methods: first-mode frequency; and a combination of input-shaping (notch-filter effect of the zero vibration) and command-smoothing (low-pass and multi-notch filtering) algorithms. The authors have presented the mathematical development of sloshing dynamics for a rectangular tank. Moreover, the fast Fourier transform was implemented to find the slosh suppression. Finally, Zang *et. al.* [16] successfully eliminated the transient and residual slosh induced by several collaborations of driving motions and fluid depths[16].

III. Methodology

This section covers a mathematical model for sloshing phenomena derived inside a liquid-filled container that moves along a 3D space. By linearizing the NavierStokes equations a linear model can be obtained. Furthermore, it also discusses the implementation of a Model-Based suppression control that enables the DRC-Hubo to climb a staircase with lower sloshing rate.

A. Slosh Dynamics

Consider the water bucket (bare wall cylindrical tank) on Figure 2 assuming that the boundary conditions at the wall and bottom for cylindrical coordinates are:

$$\left.\frac{\partial \Phi}{\partial r}\right|_{r=R} = 0 \ , \left.\frac{\partial \Phi}{\partial z}\right|_{z=-h} = 0$$

Authorized licensed use limited to: INDIAN INSTITUTE OF TECHNOLOGY ROORKEE. Downloaded on February 15,2021 at 10:02:51 UTC from IEEE Xplore. Restrictions apply.

Where Φ is total velocity potential function, and r and z are the respective radius and height. Then a possible fundamental general solution is showed at equation below Eq.1. Thus, λ_{mn} and β_{mn} are the free surface initial conditions that varies with time of the nth sloshing mode (modal analysis of a liquid free-surface motion) in the bucket, $J_m(\lambda_{mn}\, r)$ is a first kind Bessel function of order m, and λ_{mn} are the roots of $\frac{\partial J_m(\lambda_{mn}\, r)}{\partial r}\Big|_{r=R} = 0$ [17].

$$\Phi(r,\theta,z,t) = \sum_{m=0}^{\infty}\sum_{n=1}^{\infty}\Big[\alpha_{mn}(t)\, cos(m\,\theta) + \beta_{mn}(t)\, sin(m\,\theta)\Big]\, J_m(\lambda_{mn}\, r)\, \frac{cosh[\lambda_{mn}(z+h)]}{cosh[\lambda_{mn}\, h]} \quad (1)$$

Hence, if λ_{mn} and β_{mn} are harmonic functions, such as $sin(\omega_{mn}\, t)$ then we can obtain the natural frequency of the liquid after using Laplaces equation through Eq.2. Please note that the vertical velocity of a fluid $z = \eta(r,\theta,t) = \eta(x,y,t)$ is known as the kinematic free-surface condition used to obtain the wave height η given by Eq.3.

$$\omega_{mn} = \sqrt{\frac{g\,\xi_{mn}}{R}\, tanh\Big(\frac{h\,\xi_{mn}}{R}\Big)} \quad (2)$$

Where R is the cylinder radius, g is gravity ($9.81 m/s^2$), h is the liquid height, and ξ_{mn} is the root of the derivative of the Bessel function of the first kind (which will later be treated as the damping ratio). Now, on Fig.2 the dashed circle represents the waive oscillation, which for modeling of planar sloshing is extreme important. Therefore, according to Ibrahim[17] for a cylindrical bucket the wave height at the wall η_w can be expressed by Eq3. Where Ω and X_0 are excitation frequency and amplitude respectively.

$$\eta_w = \frac{2\,\Omega^2\, R}{g}\, \frac{\omega_n^2\, X_0\, sin(\Omega\, t)}{(\xi_{1n}^2 - 1)\,(\omega_n^2 - \Omega^2)} \quad (3)$$

B. Spherical Pendulum Method

At this moment a pendulum modeling is appropriate, knowing that an ordinary pendulum's natural frequency can be expressed by $\omega_{mn} = \sqrt{g/l}$ we could then express the length of the pendulum.

$$l_n = \frac{R}{\xi_{1n}}\, tanh\Big(\frac{\xi_{1n}\, h}{R}\Big) \quad (4)$$

where the roots for first mode(diameter perpendicular to the direction of rocking bucket).

In order to model a spherical pendulum equation of motion the Lagrange equation ought to be used. Thus, kinetic and potential energies in terms of θ and ψ are illustrated on Eq.5 and Eq.6 respectively(Fig.2)[18]. In addition, K and PE are derived based on the equations of motion of the spherical pendulum $x(t) = X_0\, cos(\Omega\, t)$.

$$K = \frac{m_1}{2}\,[(l_1\,\dot{\psi}\, sin\theta - \dot{x}\, sin\psi)^2 + (l_1\,\dot{\theta} + \dot{x}\, cos\psi\, cos\theta)^2] \quad (5)$$

$$PE = m_1\, g\, l_1\, (1 - cos\theta) \quad (6)$$

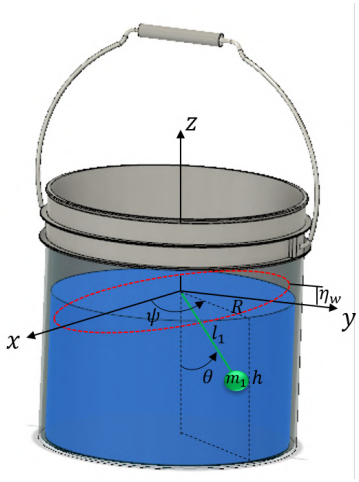

Fig. 2: Sloshing dynamics model for a spherical pendulum of a filled fluid container (m_1 is the mass of the body of water)

Moreover, by applying Lagranges function $\mathcal{L} = K - PE$ and adding the damping ratio ζ [18]:

$$\ddot{\theta} + sin\theta\,(\omega_{1_n}^2 - \dot{\psi}^2\, cos\theta) + 2\,\zeta\,\omega_{1n}\,\dot{\theta} + \frac{\ddot{x}}{l_1}\, sin\psi = 0 \quad (7)$$

where the general equation of motion is given by:

$$\ddot{\theta} + 2\,\omega_{1n}\,\zeta\,\dot{\theta} + \omega_{1_n}^2\,\theta = \frac{\ddot{x}}{l_1} \quad (8)$$

For the damping ratio an empirical equation (Eq.9) is needed, and it can be obtained through the equation bellow in terms of the kinematic viscosity ν, bucket radius R and the height of the fluid h [19]. As mentioned previously, since $1 > \zeta$ the system has underdamped behavior.

$$\zeta \approx 0.52\,\sqrt{\frac{\nu}{\sqrt{R^3}}}\left[1 + \frac{0.32\,(R-h)}{R\, sinh(\frac{1.18\,h}{R})\, cosh(\frac{1.18\,h}{R})}\right] \quad (9)$$

C. Slosh Mitigation Controller

Preliminary work with DRC-Hubo carrying rigid and non-rigid uses a modified Linear Inverted Pendulum Model (LIPM) for locomotion[13]. In contrast, this paper focuses more on the control and data acquisition related to the overall movement of the arms which by nature causes external disturbances on the water buckets. Most importantly, although the containers' force influences the humanoid's whole-body dynamical behavior, they are not enough to change the center of gravity (CoG) of the robot in an unstable manner. As a result, Gazebo simulations were performed to guarantee stability of the CoM/CoG during stair climbing. Thus, the arms have a strict adjustment range of $4cm$ on the x and y axes (Fig.5, Left), restraining the arms to move outside of the designated motion plane, and therefore securing a safe "stair climb" locomotion.

Figure 3 depicts the full controller diagram. Hence, the sloshing mitigating controller is mainly composed of a full

Authorized licensed use limited to: INDIAN INSTITUTE OF TECHNOLOGY ROORKEE. Downloaded on February 15,2021 at 10:02:51 UTC from IEEE Xplore. Restrictions apply.

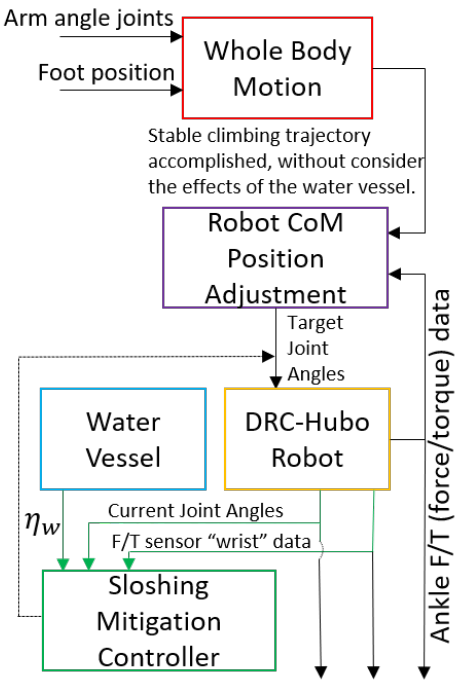

Fig. 3: Controller block diagram

state feedback PID controller with a 0.004% steady state error, and 0.169 sec settling time. The input is the the current joint angles, wave height η_w, and F/T(force and torque) data of the wrist. Therefore, through the position of the angle the overall acceleration in the x-axis $\ddot{x}$ is calculated based on the pendulum dynamic model $\ddot{\theta}$ which can be approximated by Eq.8. Furthermore, the output are the new target joint angle positions which the arm has to adjust itself to auto-correct for the sloshing disturbance. Conclusively, a summary of the main parameters used are displayed on Table I.

TABLE I: Principle Parameters

Parameter	Value	Unit	Equations
Water level	$h = 0.09$	m	(1)(2)(3)(9)
Vessel radius	$R = 0.12$	m	(2)(3)(4)(9)
Water kinematic viscosity	$\nu = 1.004e-6$	m/s^2	(9)
Damping ratio	$\zeta \approx 2.62e-3$		(9)
Pendulum's length	$l_1 \approx 0.09$	m	(3)
Natural frequency	$\omega_{1n} \approx 0.0218$	Hz	(2)
Mass of water	$m_1 = 3.78$	Kg	(5)(6)

D. System integration

Figure 4 depicts the system architecture for the proposed application. Once the water bucket is securely coupled, DRC-Hubo can read force/torque data through FT sensors and the joint encoder will monitor the actuators real positions. The green section of Fig.4 which is called PODO (software that DRC-Hubo uses to communicate with the programs, sensors, simulator, and user) is responsible for sending motor commands to the controllers for climbing stairs and arm. In addition, the robot state publisher is responsible for the exact joint position during operation. The diagram also demonstrates how the input from the water container interacts with the humanoid hardware. The system has been encapsulated by using ROS (Robot Operating System) nodes to generate the climbing and arm controller inputs.

TABLE II: DRC-Hubo simplified specifications.

Spec	DRC-Hubo
DoF	32
Weight (Kg)	80
COM height (m)	0.7752
Total height (m)	1.67
Arm link length (m)	0.848

IV. Experimentation

This section will present an overview of how the controller was tested, as well our experiment setup. For real world experiments DRC-Hubo was used to verify the effectiveness of our sloshing suppression controller. Table II depicts the fundamental characteristics for DRC-Hubo.

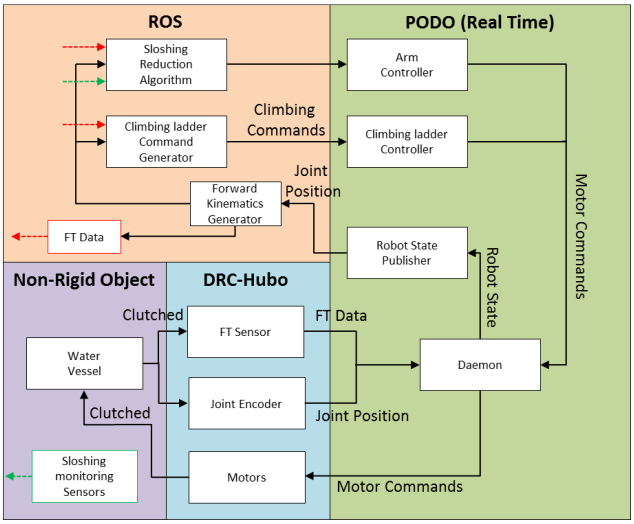

Fig. 4: System integration diagram illustrating the four main sectors; PODO, Humanoid, Non-rigid body and ROS

Figure 5 shows a side-by-side comparison between the Gazebo simulation and the actual experimentation. The metal staircase has three steps and each step is $h_s = 23cm$ tall, $w_s = 29cm$ wide and $l_s = 108cm$ long.

The containers used are $h_b = 23.445cm$ high and with a radius of $R = 12cm$. Additionally, eTape liquid level sensors and an accelerometer were used to evaluate the sloshing on the buckets by monitoring η_w (wave height at the wall, Sec.III-A). These eTapes (Fig.6(b)) are solid-state sensors manufactured by Adafruit and programmed through Arduino for the sole purpose of data acquisition. The accelerometer was used to evaluate the overall motion of the bucket (Fig.6(a)), particularly the acceleration in the x-axis.

Authorized licensed use limited to: INDIAN INSTITUTE OF TECHNOLOGY ROORKEE. Downloaded on February 15,2021 at 10:02:51 UTC from IEEE Xplore. Restrictions apply.

Finally, upon setting the robot in the "climb ready" position (Fig.5) DRC-Hubo is then placed in front of the staircase at $12.5cm$ from the first step. The sensors for data acquisition (eTape) and the container acceleration are activated through ROS. There are three layers of operation in order to conduct the experiment: First, Hubo's main computer runs the modified algorithm to climb the stairs; Second, the main computer uses the acceleration data which is being fed via ROS; Third, the operator must initiate the experiment through the GUI (main computer) after the insertion of certain parameters (distance between feet and 3/4 of the end of the first step length). Hence, the robot can commence its motion once these three layers are working together.

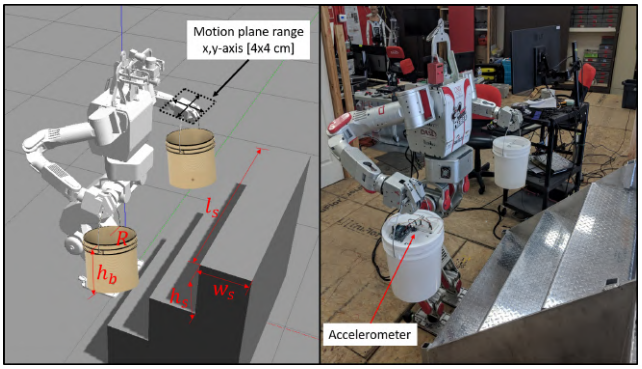

Fig. 5: **Left** - Gazebo simulation concept, highlighting the real stair dimensions. **Right** - Real world experiment with DRC-Hubo on standby prior the the experiment

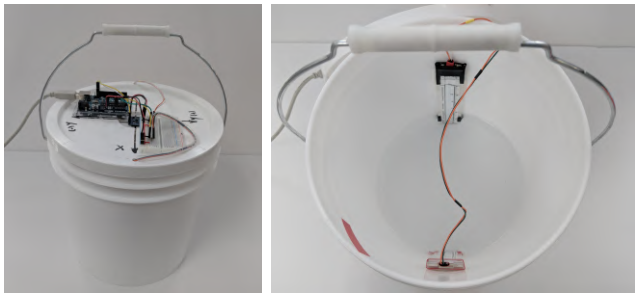

(a) Outside view (b) Inside view

Fig. 6: Physical bucket used for data acquisition (1 gallon was used during experiments out of a 2 gallons maximum capacity vessel)

V. Results

This section will compile the results collected through simulations as well as real world experiments. After the mathematical model for the spherical pendulum was defined the design of the controller becomes relatively simple.

In order to verify the sloshing reduction the data collected from the eTape was used. It is important to point out that the eTape has limited accuracy of $0.1cm$, however upon several tests it has been found that the error is of $\pm 0.4cm$. Therefore, Figure 7 depicts the sloshing while DRC-Hubo is climbing the stairs.

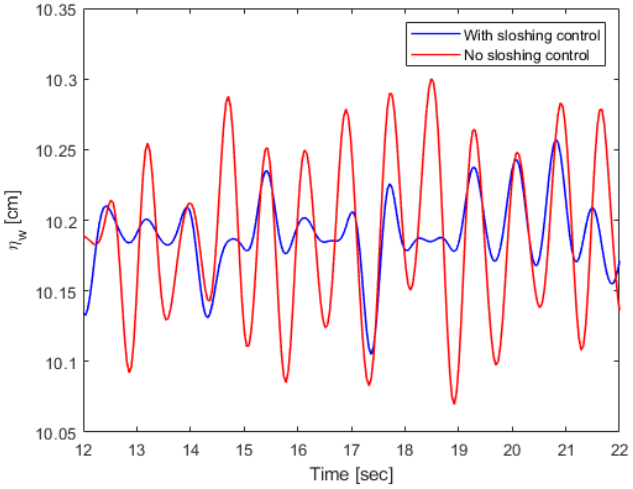

Fig. 7: Filtered sloshing data compiled before and after the implementation of the sloshing reduction controller (sampling rate 200 Hz)[1]

The initial water level inside of the container is $9cm$, however the eTape registered $\approx 9.8cm$ initially due to a slack at the bottom of the bucket. The blue curves signify the sloshing prior the PID controller was implemented, whereas orange represents the sloshing behavior after the control implementation. Hence the proposed controller indeed improves the sloshing suppression by reducing the sloshing waves η_w to an average of $\approx 0.8cm$. To evaluate the data accuracy each eTape was treated separately. Fig.7 shows high spikes downwards reaching the $8.61cm$; this is due to data from the eTape at the positive x-axis (Fig.6) being more sensitive to decreases of height. Thus, upon testing the hardware and comparing the results the sloshing is better represented by the downward peaks. It is important to mention that all the experiments were conducted with the water container half full (3.78 liters), due to the limitations of the robot's manipulators. Furthermore, the experiment was conducted 42 times to validate the proposed controller. Ultimately, Figure 8 depicts one of the experiment trials with the use of the sloshing control on the full-sized humanoid DRC-Hubo.

VI. Conclusion And Future Work

This paper successfully developed and tested a control system for sloshing suppression of water containers being carried by a full-sized humanoid robot. The controller chosen worked accordingly by reducing the sloshing wave length by an average of $0.8cm$, which was implemented by modeling the spherical pendulum applied to fluid sloshing dynamics. Several trials were performed in order to tune the controller, because the output is end-effector position the controller is not very effective. In contrast, if the counter force was

[1]Please, watch the Full HD video of the experiments at `https://youtu.be/c_htRuBwOdk`.

Authorized licensed use limited to: INDIAN INSTITUTE OF TECHNOLOGY ROORKEE. Downloaded on February 15,2021 at 10:02:51 UTC from IEEE Xplore. Restrictions apply.

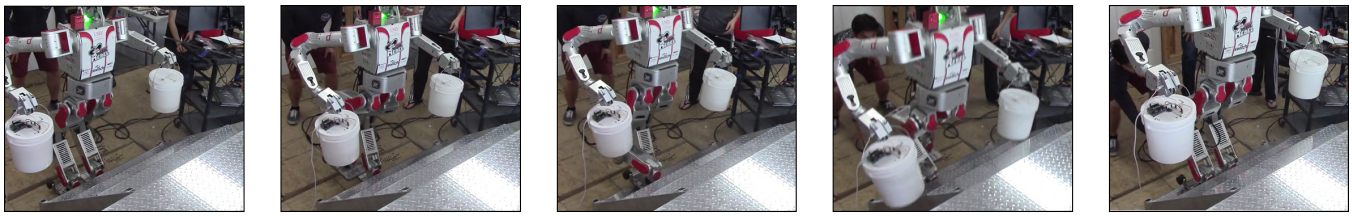

(a) (b) (c) (d) (e)

Fig. 8: DRC-Hubo performing stair climbing using the Model-Based suppression control

applied on the actual bucket the sloshing could have been mitigated further. In addition, because the bucket is not rigidly coupled with the bucket body a proper sloshing suppression is extremely convoluted. Finally, even though a sloshing reduction was achieved, a further approach would be to develop a container that has a sloshing suppression mechanism of its own. Therefore, future work will be to design a container with stepper motors and the controller embedded inside the container. Therefore, any humanoid could carry the container with minimum spillage. Furthermore, for future work the sloshing suppression on the current system might be improved by using a more sophisticated controller. For instance, an active force control (AFC) method was considered which generates "auto-correct" commands to the arm as the robot climbs the stairs based on force torque (FT) data. Furthermore, in the future the authors would like to increase the robot's load carrying capabilities. In conclusion, the authors have showed a full-sized humanoid successfully climbing stairs while carrying water vessels.

ACKNOWLEDGMENT

The authors gratefully acknowledge the contributions of Dylan Wallace, Norberto Torres Reyes, Keitaro Nishimura, Yu Hang He, Mike Clark and Dr William Culbreth at the University of Nevada, Las Vegas.

REFERENCES

[1] L.C. Pullen, "Puerto Rico after Hurricane Maria,"*American Journal of Transplantation,* pp. 283-284, February, 2018.

[2] G. Pratt and J. Manz, *"The DARPA Robotics Challenge,"* IEEE Robotics & Automation Magazine, pp. 1012, 2013.

[3] M. Schwarz, T. Rodehutskors, D. Droeschel, M. Beul, M. Schreiber, N. Araslanov, I. Ivanov, C. Lenz, J. Razlaw, S. Schller and D. Schwarz, "NimbRo rescue: Solving disasterresponse tasks with the mobile manipulation robot momaro,"*Journal of Field Robotics,* pp. 400-425, March, 2017.

[4] G.C. Haynes, D. Stager, A. Stentz, J.M. Vande Weghe, B. Zajac, H. Herman, A. Kelly, E. Meyhofer, D. Anderson, D. Bennington and J. Brindza, "Developing a robust disaster response robot: CHIMP and the robotics challenge,"*Journal of Field Robotics,* pp. 281-304, March, 2017.

[5] P. Oh, K. Sohn, G. Jang, Y. Jun and B.K. Cho, "Technical Overview of Team DRCHubo@ UNLV's Approach to the 2015 DARPA Robotics Challenge Finals,"*In Journal of Field Robotics,* pp.874-896, March, 2017.

[6] S.Y Shin and C. Kim, "Human-like motion generation and control for humanoid's dual arm object manipulation," *In IEEE Transactions on Industrial Electronics,* pp. 2265-2276, 2015.

[7] I.G. Ramirez-Alpizar, M. Naveau, C. Benazeth, O. Stasse, J.P. Laumond, K. Harada and F. Kanehiro, "Motion generation for pulling a fire hose by a humanoid robot," *In Humanoid Robotics (Humanoids),* pp. 1016-1021, Cancun, Mexico, November, 2016.

[8] S. Miller, J. Van Den Berg, M. Fritz, T. Darrell, K. Goldberg and P. Abbeel, "A geometric approach to robotic laundry folding,"*In The International Journal of Robotics Research,* pp.249-267, February, 2012.

[9] J. Ortiz and A. Barhorst, "Closed-form modeling of fluid-structure interaction with nonlinear sloshing: potential flow,"*In AIAA journal,* pp.1510-1517, September, 1997.

[10] W. Aribowo, T. Yamashita and K. Terashima, "Integrated trajectory planning and sloshing suppression for three-dimensional motion of liquid container transfer robot arm,"*In Journal of Robotics,* p.3, January, 2015.

[11] M. Reyhanoglu and J.R. Hervas, " Nonlinear modeling and control of slosh in liquid container transfer via a PPR robot,"*Communications in Nonlinear Science and Numerical Simulation,* pp.1481-1490, June, 2013.

[12] L. Moriello, L. Biagiotti, C. Melchiorri and A. Paoli, "MControl of liquid handling robotic systems: A feed-forward approach to suppress sloshing," *In Robotics and Automation (ICRA),* pp. 4286-4291, Singapore, Singapore, May, 2017.

[13] J.C. Vaz, H. Lee, Y. Jun and P. Oh, "Towards tasking humanoids for lift-and-carry non-rigid material," *In Ubiquitous Robots and Ambient Intelligence (URAI),* pp. 316-321, Jeju, South Korea, May, 2017.

[14] J.P. Mishra and S.R. Kurode, "A robust control approach for suppression of container-slosh using output-feedback based on super-twisting algorithm,"*In International Journal of Advanced Mechatronic Systems,* pp.24-35, January, 2014.

[15] D.S. Purnomo, A.R.A. Besari and Z. Darojah, "Control of Liquid Sloshing Container using Active Force Control Method," *In IOP IAES International Conference on Electrical Engineering, Computer Science and Informatics,* p.012007, Semarang, Indonesia, April, 2017.

[16] Q. Zang, J. Huang and Z. Liang, "Slosh suppression for infinite modes in a moving liquid container,"*In IEEE/ASME Transactions on Mechatronics,* pp.217-225, February, 2015.

[17] R.A. Ibrahim, "Liquid sloshing dynamics: theory and applications," *Cambridge University Press,* May, 2005.

[18] D.D. Kana, "A model for nonlinear rotary slosh in propellant tanks,"*In Journal of Spacecraft and Rockets,* pp.169-177, March, 1987.

[19] H.N. Abramson, "The dynamic behavior of liquids in moving containers, with applications to space vehicle technology," *National Aeronautics and Space Administration(NASA) publications,* 1966.

[20] Y. Izawa, T. Osaki, K. Kamiya, S. Fujii, N. Misawa, S. Takeuchi and N. Miki, "Suppression of sloshing by utilizing surface energy and geometry in microliter cylindrical well,"*Sensors and Actuators B: Chemical,* pp.1036-1041, April, 2018.

Authorized licensed use limited to: INDIAN INSTITUTE OF TECHNOLOGY ROORKEE. Downloaded on February 15,2021 at 10:02:51 UTC from IEEE Xplore. Restrictions apply.